Journal of Materials Chemistry C

Accepted Manuscript

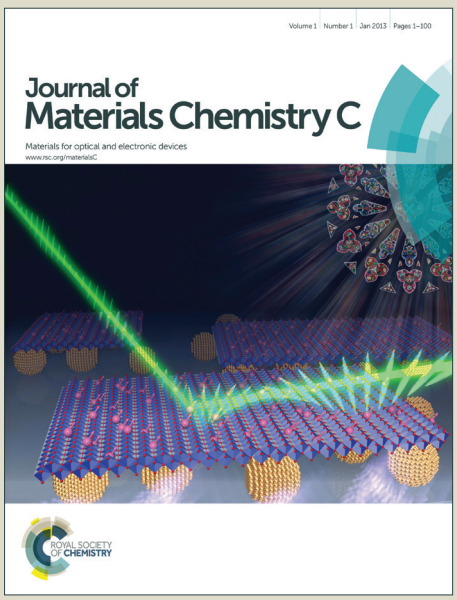

ROYAL SOCIETY OF CHEMISTRY

www.rsc.org/materialsC

Journal of Materials Chemistry C

Journal of Materials Chemistry C

Cite this: DOI: 10.1039/c0xx00000x

www.rsc.org/xxxxxx

ARTICLE TYPE

A Novel Tetraphenylsilane-Phenanthroimidazole Hybrid Host Material for Highly Efficient Blue Fluorescent, Green and Red Phosphorescent OLEDs

Dong Liu, Mingxu Du, Dong Chen, Kaiqi Ye, Zuolun Zhang,* Yu Liu* and Yue Wang

Received (in XXX, XXX) Xth XXXXXXXXX 20XX, Accepted Xth XXXXXXXXX 20XX
DOI: 10.1039/b000000x

A novel organosilane compound, bis(4-(1-phenylphenanthro[9,10-d]imidazol-2-yl)phenyl)diphenylsilane ($Si(PPI)_2$), has been designed and synthesized. It has a high thermal decomposition temperature of 528 °C and is able to form an amorphous glass with a high glass-transition temperature of 178 °C. In addition, it possesses high singlet and triplet energies and displays efficient energy transfer to the selected blue fluorescent and green and red phosphorescent dopants when used as a host material. Electrochemical measurements and single-carrier devices indicate that $Si(PPI)_2$ is a bipolar transport material, allowing the injection and transport of both electrons and holes. By using ($Si(PPI)_2$) as a host, high-performance fluorescent blue (**FB**) and phosphorescent green (**PG**) and red (**PR**) OLEDs with an uniform and simple device configuration have been achieved. These OLEDs exhibit very high peak external quantum efficiency (EQE) and peak power efficiency (PE), *i.e.* 6.1% & 8.0 lm W^{-1} for **FB**, 19.2% & 51.1 lm W^{-1} for **PG** and 12.0% & 15.6 lm W^{-1} for **PR**. Moreover, the high-level EQE of 4.0, 19.1 and 10.6% and PE of 3.0, 41.6 and 7.5 lm W^{-1} can be maintained by **FB**, **PG** and **PR**, respectively, at the practical luminance of 100 cd m^{-2}. Furthermore, the emission colors of these OLEDs remain almost unchanged within the whole range of driving voltages. Importantly, the blue OLED displays the pure blue emission (CIE: 0.18, 0.17).

Introduction

Organic light-emitting diodes (OLEDs) have attracted considerable scientific and industrial interests since the pioneering work by Tang et al. in 1987.[1] Generally, the phosphorescent OLEDs (PhOLEDs), in which the emitting layers (EML) are normally constructed by doping the phosphors into charge-transport hosts, have much higher electroluminescent (EL) efficiency than the conventional fluorescent OLEDs, due to the radiative harvesting of both electro-generated singlet and triplet excitons.[2,3] Recently, green and red PhOLEDs with 100% internal quantum efficiency have been reported,[4–7] but high performance blue PhOLEDs have not yet to be achieved, which are subject to the sky-blue emission with the Commission International de I' Eclarirage (CIE) coordinates of x and/or y ≥ 0.20 and their instability in emission color and EL efficiency.[8–12] It has become a bottleneck in the development of efficient OLEDs in both flat-panel displays and solid-state lighting. Furthermore, the approximate 0.5-1.0 eV exchange energy losses in power efficiency resulted from the energetic relaxation following intersystem crossing from the conductive host into the blue emissive triplet state represent another drawback.[13] Considering these issues regarding the blue PhOLEDs, adopting the stable blue fluorescent emitters to realize high-quality blue EL emission is a complementary effective strategy and becomes again an active research area.[14-17] On the other hand, blue, green and red emitters often require different hosts to achieve highly efficient energy transfer from host to emitter[18–22] Therefore, the full-color and white OLEDs were often established based on a complex material system and, correspondingly, high-cost organic syntheses.. In this sense, achieving high performance blue, green and red electroluminescence through a simple material system with the aim to reduce the production cost of materials and simplify the manufacturing process is an important issue for OLED applications. Given this, many efficient multi-color and white PhOLEDs based on a universal host have been achieved in the literature.[23–26] However, designing and synthesizing an organic molecule that can be employed as a host to realize the efficient blue fluorescent OLEDs as well as phosphorescent OLEDs with the relatively long-wavelength light, such as green and red, has not been reported previously, and is still a considerable challenge.

Organic derivatives and metal complexes of phenanthroimidazole (PPI) have been widely utilized as blue fluorescent emitters and/or the host materials for highly efficient OLEDs,[27–32] due to their high-energy emission and bipolar transport properties. Additionally, tetraarylsilane compounds have attracted a fair amount of attention as organic EL materials, attributed to their wide bandgap and the high thermal stability resulted from their non-conjugated tetrahedral molecular geometry.[25,33–37] In this contribution, by integrating one

tetraphenylsilane and two PPI groups, we have prapared bis(4-(1-phenylphenanthro[9,10-d]imidazol-2-yl)phenyl)diphenylsilane ($Si(PPI)_2$) with the expectation that this compound could have good thermal stability, high-energy emission and good carrier-transport ability to work as a high-performance host material. We have found that, through doping fluorescent blue or phosphorescent green or red emitters into $Si(PPI)_2$, a series of host-guest systems with efficient energy transfer can be realized. They showed very high peak external quantum efficiency (EQE) and power efficiency (PE) values of 5.6% & 8.0 lm W^{-1} for blue emission with the CIE coordinates of (0.18, 0.17), which are among the highest EL efficiencies ever reported for the pure blue fluorescent OLEDs that meet the standard of the $CIE_{x,y}$ coordinates of x≤0.20 and y≤0.20, as well as 18.8% & 51.1 lm W^{-1} for green emission and 11.9% & 15.6 lm W^{-1} for red emission. They maintain the high level of 3.6, 18.7 and 10.5% & 3.0, 41.6 and 7.5 lm W^{-1} at the practical luminance of 100 cd m^{-2} respectively, and their EL emission color remain almost unchanged within the whole range of the corresponding driving voltages.

We will present a comprehensive investigation on $Si(PPI)_2$, which not only encompasses its thermal, photophysical and electrochemical properties, but also the emphatically studies on its carrier injection/transport abilities and EL characteristics as host material.

Experimental section

General information

The auxiliary materials such as 1,4-bis[(1-naphthylphenyl) amino]-biphenyl (NPB), 4,4′,4″-tri(*N*-carbazolyl) triphenylamine (TCTA), 1,3,5-tris(N-phenylbenzimidazol-2-yl)benzene (TPBi), and the series of emitting fluorescent/phosphorescent materials including $An(PPI)_2$,[38] $Ir(ppy)_3$,[3] and $(bt)_2Ir(dipba)$[39] (**Fig. 5**) for fabricating the OLEDs were prepared according to literature procedures and purified further by vacuum sublimation prior to use. Starting materials for synthesis were obtained from commercial suppliers and used without further purification. Anhydrous THF was distilled with sodium benzophenone ketyl under nitrogen atmosphere and degassed by the freeze-pump-thaw method. All glasswares, syringes, magnetic stirring bars and needles were dried in a convection oven for at least 4 hours. Reactions were monitored with thin layer chromatography (TLC). Commercial TLC plates (Silica gel 60 F254, Merck Co.) were developed and the spots were seen under UV light at 254 and 365 nm. Silica column chromatography was done with silica gel 60 G (particle size 5~40 μm, Merck Co.). ^1H NMR spectra were recorded on a Bruker AVANCE 300 MHz spectrometer with tetramethylsilane as an internal standard. Mass spectra were measured on a GC/MS system. Elemental analyses were performed on a flash EA 1112 elemental analyzer. IR spectra were recorded on a Bruker VERTEX 80v spectrometer. UV-vis absorption spectra were obtained using a Shimadzu UV-2550 UV-vis spectrometer. Photoluminescent (PL) spectra were recorded on a Perkin-Elmer LS-55 fluorescence spectrometer with a Xe arc lamp excitation source. Solid state PL efficiencies were measured using an integrating sphere (C-701, Labsphere Inc.), with a 365 nm Ocean Optics LLS-LED as the excitation source, and the light was introduced into the integrating sphere through optical fiber. Time-resolved fluorescence spectra were collected on an Edinburgh mini-τ fluorescence lifetime spectrometer, with an Edinburgh EPL-405 picosecond pulsed diode laser as the excitation source. Electrochemical measurements were performed with a BAS 100W Bioanalytical electrochemical workstation, using a Pt disk as working electrode, platinum wire as auxiliary electrode, and a porous glass wick Ag/Ag^+ as pseudo-reference electrode with standardized against ferrocene/ferrocenium. A 0.1 M solution of *n*-Bu_4NPF_6 in CH_2Cl_2 (for oxidation) or DMF (for reduction) was used as the supporting electrolyte. A scan rate of a 100 mV s^{-1} was adopted. All the redox potentials are given against ferrocene/ferrocenium.

Fabrication of the OLEDs and EL measurements

The general architecture of the complex multilayer diodes used in this study is as follows: The ITO (indium-tin oxide) coated glass substrates (20Ω/square) were pre-cleaned carefully in ethanol, followed in acetone with the soap ultrasonic bathes and treated by UV/O_3 for 2 min. The devices were prepared in vacuum at a base pressure around 5 × 10^{-6} Torr. All organics were thermally evaporated at a rate of 1.0 Å s^{-1} at a base pressure of around 3.5 x 10^{-4} Pa. A LiF layer (0.5 nm) was deposited at a rate of 0.2 Å s^{-1}. The finishing Al electrode (cathode) was deposited at a rate of 10 Å S^{-1} in another chamber. The thicknesses of the organic materials and the cathode layers were controlled using a quartz crystal thickness monitor. The electrical characteristics of the devices were measured with a Keithley 2400 source meter. The EL spectra and luminance of the devices were obtained on a PR650 spectrometer. All the devices fabrication and device characterization steps were carried out at room temperature under ambient laboratory conditions. Current-Voltage characteristics of single-carrier devices were measured using the same semiconductor parameter analyzer as for OLED devices.

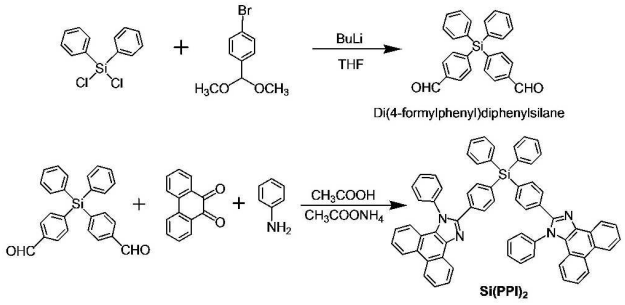

Synthesis

Scheme 1. Synthetic procedure and structures of $Si(PPI)_2$.

The synthetic route of $Si(PPI)_2$ is shown in **Scheme 1.**

Di(4-formylphenyl)-diphenylsilane:[40] *n*-BuLi (1.6 M in hexane, 20 mL, 32 mmol) was added slowly to a THF(120 mL) solution of 4-bromobenzaldehyde dimethyl acetal (7.40 g, 32 mmol) at -78 °C, and then the mixture was stirred at this temperature for 1 h. After dichlorodiphenylsilane (1.52 mL, 12.5 mmol) was added, the reaction mixture was stirred at -78 °C for 1 h, slowly warmed to r.t., stirred for 12 h at r.t., quenched with 2 N HCl and extracted with ether. The organic phase was washed

with brine and dried over $MgSO_4$, and then the solvent was evaporated under reduced pressure. To the obtained residue, acetic acid (10 mL) and H_2O (3 mL) were added, and the obtained mixture was stirred for 3 h at r.t., poured into saturated aqueous $NaHCO_3$ and extracted with ether. The extracts were washed with brine, dried over $MgSO_4$, filtered and concentrated under vacuum. The obtained residue was purified by column chromatography (silica gel, hexanes/EtOAc 4:1) to give the product as white solid (2.85 g, 58%). ^{1}H NMR (300 MHz; $CDCl_3$; Me_4Si): δ 10.01 (s, 2H), 7.89 (d, J = 8.0 Hz, 4H), 7.74 (d, J = 8.0 Hz, 4H), 7.56–7.40 (m, 10H).

Bis(4-(1-phenylphenanthro[9,10-d]imidazol-2-yl)phenyl) diphenylsilane (Si(PPI)$_2$): Reflux the mixture of 9,10-phenanthrenequinone (312 mg, 1.5 mmol), Di(4-formylphenyl)-diphenylsilane (294 mg, 0.75 mmol), aniline (0.55 mL), ammonium acetate (1.16 g, 15 mmol) and glacial acetic acid (30 mL) for 24 h. After cooled to room temperature, the reaction mixture was poured into stirred methanol. The precipitate was filtered, washed with methanol and dried to give the crude product, which was further purified by vacuum sublimation to provide the desired compound as white powder (414 mg, 60%). ^{1}H NMR (300 MHz, $CDCl_3$, ppm): δ 8.89 (d, J = 7.2 Hz, 2 H), 8.77 (d, J = 8.4 Hz, 2 H), 8.71 (d, J = 8.1 Hz, 2 H), 7.75 (t, J = 7.5 Hz，2H), 7.69–7.61 (m, 12H), 7.56–7.43 (m，16H)，7.37 (t ，J = 7.2 Hz，4H), 7.29–7.24 (m，2H)，7.17–7.14 (d，J = 8.1 Hz，2H). ^{13}C NMR (75 MHz, $CDCl_3$, ppm): δ 120.87, 122.84, 123.07, 124.09, 124.93, 125.66, 126.25, 127.15, 127.27, 127.91, 128.15, 128.33, 128.38, 128.48, 128.60, 128.67, 128.88, 129.07, 129.11, 129.38, 129.42, 129.53, 129.74, 129.95, 130.09, 130.20, 133.03, 133.53, 136.19, 136.38, 137.96, 138.71, 138.77. Ms *m/z*: 919.9 $[M]^+$ (calcd: 920.3). Anal.Calcd (%) for $C_{66}H_{44}N_4Si$: C, 86.05; H, 4.81; N, 6.08. Found: C, 86.38; H, 4.73; N, 6.05. IR (KBr, υ, cm^{-1}): υ= 3092, 3062, 3010, 1599, 1486, 1455, 1425, 1378, 1296, 1234, 1183, 1152, 1106, 1019, 957, 839, 804, 752, 696, 568, 506.

Results and discussion

Thermal Property

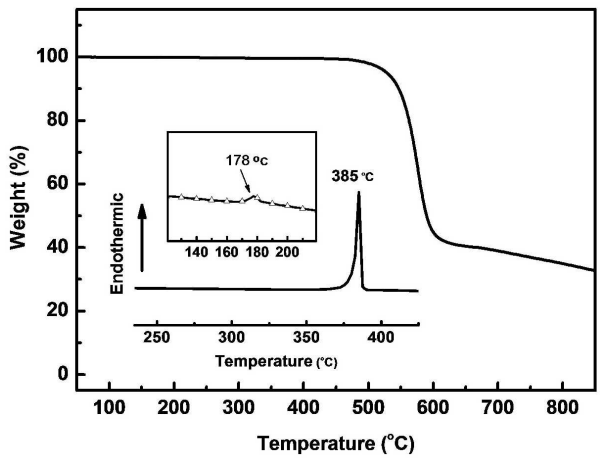

Fig. 1 TGA thermogram of Si(PPI)$_2$. Inset: DSC thermogram.

Thermal properties of Si(PPI)$_2$ was investigated using thermal gravimetric analysis (TGA) and differential scanning calorimetry (DSC) under a nitrogen atmosphere at a heating rate of 10 °C min^{-1}. The compound exhibits very good thermal stability, as evidenced by its high decomposition temperature (corresponding to 5% weight loss) of 528 °C in the TGA thermogram (**Fig.1**). This will prevent the compound from decomposing during the processes of vacuum deposition and device working. According to the DSC analysis, Si(PPI)$_2$ has a high melting point of 385 °C (**Fig.1**, **inset**). More importantly, it has an ability to form the amorphous glass with a high glass-transition temperature of 178 °C during the second-heating scan, which is beneficial to the formation of homogeneous and amorphous films upon thermal evaporation, as well as to keep the stability of the film and to decrease the phase separation of the host-guest system when Si(PPI)$_2$ is used as a host material.

Photophysical Property

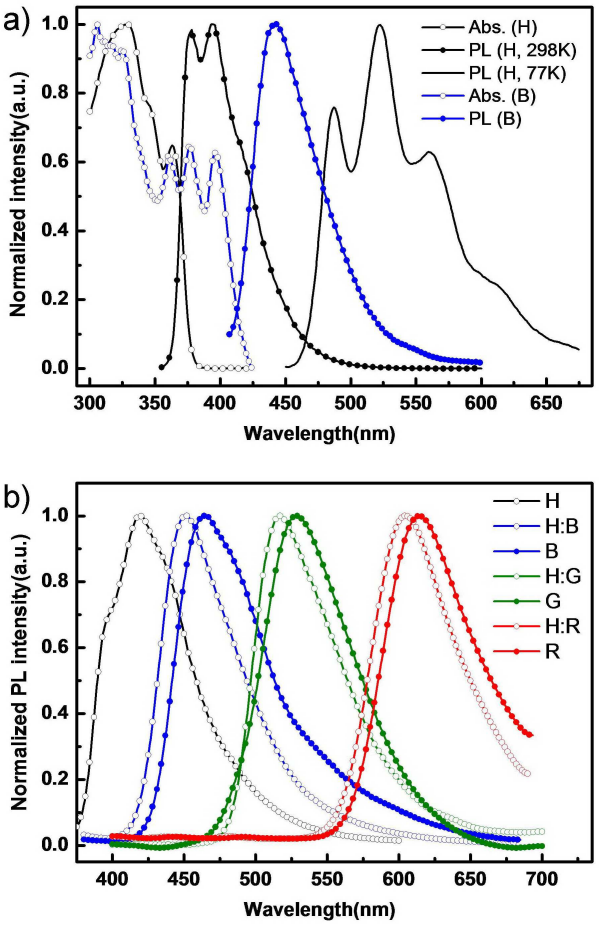

Fig. 2 a) UV-Vis absorption and PL spectra of Si(PPI)$_2$ (H) and An(PPI)$_2$ (B) measured in dichloromethane solution (5×10^{-5} M) at room temperature and the phosphorescence spectrum of Si(PPI)$_2$ in 2-MeTHF solution (5×10^{-5} M) at 77 K. b) PL spectra of the neat films of Si(PPI)$_2$ (H), blue fluophor (B), green (G) and red (R) phosphors and these dopant emitters doped in Si(PPI)$_2$ (H) thin films with 10 wt% doping concentration.

Fig. 2a displays UV-Vis absorption and photoluminescence (PL) spectra of Si(PPI)$_2$ in dichloromethane solution (5×10^{-5} M) atroom temperature (298 K) and its phosphorescence spectrum in frozen 2-MeTHF (5×10^{-5} M) at 77 K. Si(PPI)$_2$ exhibits intense deep-blue emissions in dichloromethane solution as well as in the solid film. An(PPI)$_2$ is considered to be a proper blue dopant in

our system because of its preferred pure-blue fluorescence and, importantly, a large overlap between its absorption spectrum and the solid-state emission spectrum of $Si(PPI)_2$, which may lead to efficient energy transfer from $Si(PPI)_2$ to $An(PPI)_2$. In the low-temperature (77 K) emission spectrum of $Si(PPI)_2$ **(Fig. 2a)**, a phosphorescence band showing vibrational structures can be observed. By using the highest-energy vibronic sub-band, the triplet energy (E_T) of $Si(PPI)_2$ is estimated to be 2.55 eV, which is clearly lower that of the classical blue phosphor bis[2-(4,6-difluorophenyl)pyridinato- $N,C^{2'}$](picolinato)iridium-(III) (FIrpic) (~2.65 eV)[12] and not high enough to sensitize this blue phosphor, leading to incompletely host-dopant energy transfer companied with the poor EL performance (see the Supporting Information, ESI). However, this E_T level of $Si(PPI)_2$ is sufficiently higher than those of most green and red phosphorescent emitters. This result suggests that, besides the siglet-singlet (Förster and/or Dexter) energy transfer, a triplet-triplet Dexter energy transfer can be expected when doping proper green and red emitters into $Si(PPI)_2$. The classical green phosphor $Ir(ppy)_3$ and a high-performance red phosphor $(bt)_2Ir(dipba)$ were selected as the phosphorescent dopants in this study. The PL spectra of the thin films prepared by doping respectively 10 wt% of the selected blue, green and red dopants into $Si(PPI)_2$ are measured to confirm the efficient energy transfer. As can be seen from **Fig. 2b,** all these doped films show the emission very close to those of the neat-films of respective dopants, while the emission of $Si(PPI)_2$ can not be observed. They exhibit the PL quantum efficiency values of 8±1%, 96±3% and 24±2% respectively, and their corresponding transient PL decay curves show almost single-exponential decay with the lifetimes of 3 ns, 0.97 μs and 0.71 μs at room temperature (see ESI file), indicating the complete energy transfer from the host ($Si(PPI)_2$) to three dopants. Therefore, these host-dopant systems are expected to have the potential to realize high-performance OLED devices. The slightly red-shifted emission from the doped films to the neat films of corresponding dopants should be related to the tighter packing between the dopant molecules in the neat films.

Electrochemical Property and Theoretical Calculation

Cyclic voltammetry (CV) was performed to investigate the electrochemical properties of $Si(PPI)_2$ **(Fig. 3a)**. The HOMO and LUMO energy levels were estimated to be *ca.* -5.6 eV and -2.2 eV respectively from the onsets of the oxidation and reduction potentials with regard to the energy level of forrocene (-4.8 eV[41] below vacuum). This HOMO level is much higher than those (~-7.0 eV) of previously reported the tetraarylsilane-based series of UGH host materials,[33] reflecting a better hole-injection property of $Si(PPI)_2$ due to the derivatization by the PPI group. Moreover, the HOMO level of $Si(PPI)_2$ is even higher than that of the classic fluorescent host material 4,4′-*N*,*N*′-dicarbazolylbiphenyl (CBP) (~-6.0 eV) and matches well with the most widely used hole-transporting material NPB (~-5.4 eV) and electron-blocking matertial TCTA (-5.7 eV), implying little or no hole-injection barriers from NPB or TCTA to this compound.

To gain more insight into the electronic structure of $Si(PPI)_2$, DFT calculations (B3LYP/6-31G(d)) were carried out. The HOMO is mainly distributed on one of the two phenanthroimidazole groups, with a samll contribution from the C_6H_4 group attached to it; while the LUMO is localized partly on the other phenanthroimidazole group and mainly on the C_6H_4 group between this phenanthroimidazole group and the Si atom **(Fig. 3b)**. The almost complete spatial separation of HOMO and LUMO energy levels suggests that the HOMO-LUMO excitation would shift the electron density distribution from one side of $Si(PPI)_2$ molecule as the donor to another side as the acceptor, leading to a polarized excited state. It is more important, such separation of HOMO and LUMO can provides hole- and electron-transporting channel respectively, where holes and electrons can realize intermolecular hopping smoothly along their respective conducting pathways. As thus, this is likely to result in this compound possessing bipolar charge transporting ability.[42–46]

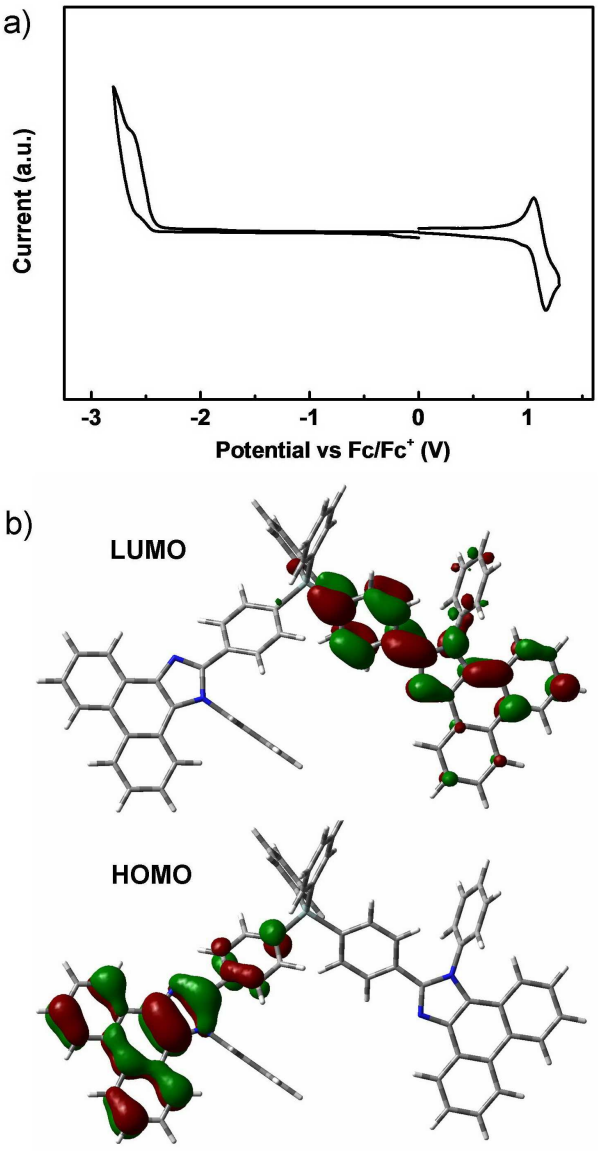

Fig. 3 a) Cyclic voltammogram of $Si(PPI)_2$ in CH_2Cl_2 for oxidation and DMF for reduction. b) Contour plots of HOMO and LUMO in $Si(PPI)_2$ from DFT calculations.

Charge carrier injection and transport properties

To further understand both hole and electron injection/transport properties of $Si(PPI)_2$, two single-carrier devices were fabricated using the following configurations: ITO/NPB (10 nm)/$Si(PPI)_2$ (30 nm)/NPB (10 nm)/Al (100 nm) (hole-only device) and ITO/TPBi (10 nm)/$Si(PPI)_2$ (30 nm)/TPBi (10 nm)/LiF (1 nm)/Al (100 nm) (electron-only device). NPB and TPBi layers are used to prevent electron and hole injection from the cathode and anode, respectively.[47-49] **Fig. 4** shows the current density versus voltage curves of both devices, respectively. It is obvious that both devices can conduct significant current, indicating that $Si(PPI)_2$ is capable of transporting both electron and hole, and exhibits its bipolar transporting nature, which is effective to balance holes and electrons in the emitting layer (EML) based on $Si(PPI)_2$. The substantially lower electron current density than the hole curve at the same voltage level should be attributed to the high-lying LUMO energy level of $Si(PPI)_2$, which means a certain injection barrier (~0.5 eV) from ETL.[32]

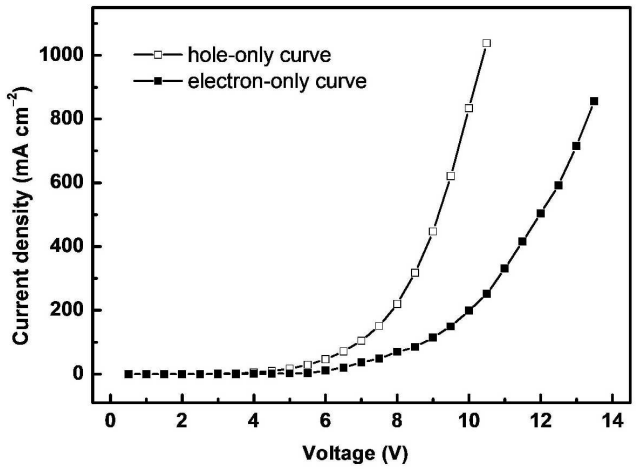

Fig. 4 Current density versus voltage characteristics of the hole-only and electron-only devices for $Si(PPI)_2$.

Characterization of fluorescent/phosphorescent OLEDs

According to above studies, $Si(PPI)_2$ could be a good host material for both fluorescent and phosphorescent OLEDs. To evaluate its practical utility, a series of OLEDs with an uniform and simple configuration of [ITO/NPB (30 nm)/TCTA (5 nm)/EML (25 nm)/TPBi (20 nm)/LiF (1 nm)/Al (100 nm)] were fabricated, and the energy diagram of the materials used in the EL devices are shown in **Fig. 5**. NPB was used as the hole-transporting material (HTL), TCTA was used as the triplet exciton-blocking layer in the PhOLEDs, and TPBi was used as the electron transport/hole-blocking layer (ETL/HBL). The films of $An(PPI)_2$, $Ir(ppy)_3$ and $(bt)_2Ir(dipba)$ doped in $Si(PPI)_2$ with the concentration of 10 wt% were adopted as the EMLs to fabricate the fluorescent blue device **FB**, the phosphorescent green and red devices **PG** and **PR** respectively. Device **FB** exhibits pure blue emissions (CIE: 0.18， 0.17) with the emission maximum at 452 nm at the luminance of 1000 cd m^{-2} (**Fig. 6**), which remains almost unchanged over a wide range of driving voltage from 3.5 V to 12 V. The EL spectrum is consistent with the PL spectrum of $An(PPI)_2$, suggesting that the blue EL emission results from the intrinsic emission of $An(PPI)_2$. On the other hand, device **PG** and **PR** present bright green and saturated red emission with the maximum peak at 516 and 612 nm and the $CIE_{x,y}$ coordinates of (0.32, 0.61) and (0.64, 0.36) respectively at the luminance of 1000 cd m^{-2}, and no additional emission from the host was observed.

Fig. 5 Energy level diagram of the materials used and the chemical structures of the emitting materials.

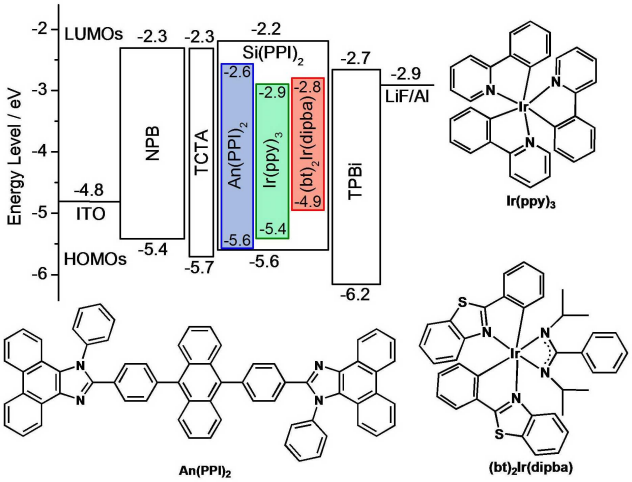

Table 2 Electroluminescent properties of the devices.[a]

Device	V_{on}/V	L_{max}/cd m^{-2}(V at L_{max})	EQE[b]/%	PE[b]/lm W^{-1}	*EL emisison peak,* CIE (x,y)[c]
FB	3.1	15000 (13.5)	6.1, 4.0, 1.9	8.0, 3.0, 0.9	452, (0.18, 0.17)
PG	3.4	60470 (12.5)	19.2, 19.1, 17.8	51.1, 41.6, 26.5	516, (0.32, 0.61)
PR	3.3	12330 (14.0)	12.0, 10.6, 7.3	15.6, 7.5, 3.3	612, (0.64, 0.36)

[a]Abbreviation: V_{on}: Turn-on voltage (Recorded at 1 cd m^{-2}). L_{max}: Maximum luminance. *EQE*: External quantum efficiency. *PE*: Power efficiency. [b]In the order of maximum, then values at 100 and 1000 cd m^{-2}. [c]Measured at 1000 cd m^{-2}.

The current density-voltage-luminance (*J-V-L*) characteristics of these OLEDs are shown in **Fig. 7a**. All these devices displayed low turn-on voltages of 3.1-3.4 V (**Table 1**), and the corresponding current density and luminance exhibited sustained increase upon increasing driving voltage. The driving voltages at the practical luminance of 100 cd m^{-2} are 5.6 V, 4.7 and 6.2 V, respectively. At driving voltages of 12.6, 9.1 and 13.5V for **FB**, **PG** and **PR** respectively, very high luminance values of >10000 cd m^{-2} were obtained. The quickly increased luminance and current density indicate a good carrier injection and transport property of the host ($Si(PPI)_2$), which is consistent with our results obtained from the single-carrier devices above. The external quantum efficiency (EQE) and power efficiency (PE) of these devices plotted with respect to the luminance are shown in **Fig. 7b,** and the EL performance data are summarized in **Table 1**. The blue device **FB** exhibited the maximum EQE and PE of 6.1% and 8.0 lm W^{-1} respectively. To the best of our knowledge, these values are among the highest EL efficiencies ever reported for the

pure blue fluorescent OLEDs that meet the standard of the $CIE_{x,y}$ coordinates of x≤0.20 and y≤0.20.[50–56] Notably, the EQE and PE values of **FB** at the brightness of 100 cd m^{-2}, which is the practical level used in the fields of display or lighting, remain as high as 4.0% and 3.0 lm W^{-1} respectively. They are much higher than those of the reference devices adopting the conventional host materials CBP or N,N'-dicarbazolyl-3,5-benzene (mCP) with the low peak EQE and PE < 1% and 2 lm W^{-1} (see ESI file). Furthermore, the green and red PhOLEDs **PG** and **PR** exhibited rather high peak EL efficiency values of 19.2, 12.0% for EQE and 51.1, 15.6 lm W^{-1} for PE. Although these EL efficiencies showed certain roll-off, the EQE values maintained the levels of 17.8% for **PG** and 7.3% for **PR** at a luminance of 1000 cd m^{-2}, and as high as 14.2, 4.6% even when the luminance reaches as high as 10000 cd m^{-2}. Obviously, in terms of the performance, these two devices are comparable with those highly efficient green and red PhOLEDs reported to date.[4-7] Such high and stable EL performance should be ascribed to the balanced carrier injection/transportability of $Si(PPI)_2$ as implied in single-carrier devices, which result in a broad distribution of recombination regions within the corresponding EMLs,[57,58] and correspondingly, a low probability of triplet-triplet annihilation that usually causes an efficiency roll-off at high current densities for the PhOLEDs. Charge confinement in the EML is another key factor for the high EL efficiency. There is large energy barriers of 0.6 eV for hole leakage from $Si(PPI)_2$ to TPBi together with the unipolar property of NPB for electron leakage from $Si(PPI)_2$ to NPB, respectively. Therefore, holes and electrons can be effectively confined inside the EML, being crucial in achieving high efficiency and low roll-off OLEDs. Besides, on the premise that the E_T (~2.55 eV) of ($Si(PPI)_2$) is high enough for working as a host, but not much higher than those of the green ($Ir(ppy)_3$, E_T: ~2.4 eV) and red ($(bt)_2Ir(dipba)$, E_T: ~2.1 eV) phosphorescent dopants, the energy loss during the host-to-dopant energy transfer process can be reduced as far as possible. It is notable that the excellent performances of all our blue, green and red OLEDs were obtained from the same device configuration through adopting a same host material. The simple material system and the easily controlled fabrication process are of significance and importance for reducing the cost and enhancing the process stability in commercial mass production.

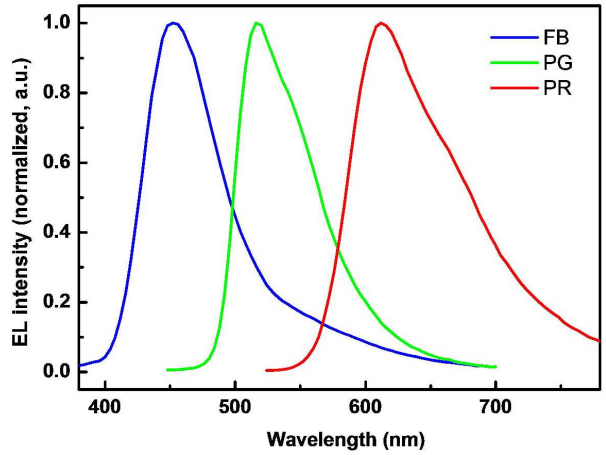

Fig. 6 EL spectra of devices **FB**, **PG** and **PR** at the luminance of 1000 cd m^{-2}.

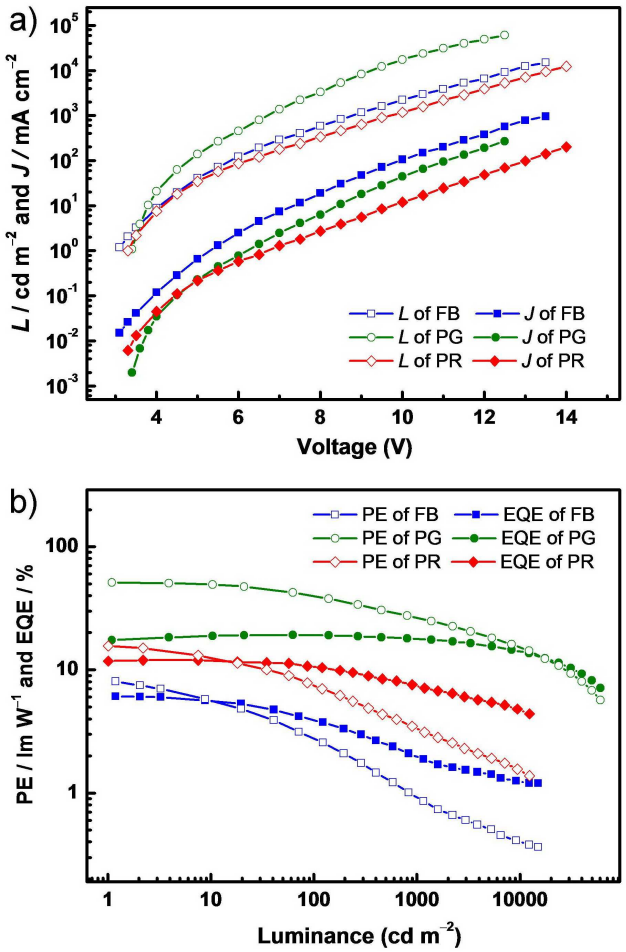

Fig. 7 Current density-voltage-luminance (*J-V-L*) curves (a) and power efficiency (PE)-luminance-external quantum efficiency (EQE) curves (b) of devices **FB**, **PG** and **PR**.

Conclusions

In summary, we have developed a novel tetrahenylsilane-phenanthroimidazole hybrid compound, $Si(PPI)_2$, which can act as a host that realizes the highly efficient blue fluorescent OLEDs as well as green and red phosphorescent OLEDs by adopting an uniform and simple device configuration. The pure-blue device with the CIE coordinates of (0.18, 0.17) exhibited the maximum EQE and PE of 6.1% and 8.0 lm W^{-1}, respectively, which are among the highest EL efficiencies ever reported for pure-blue devices. Furthermore, the EL performance of our green and red phosphorescent devices is also comparable with that of the most efficient green and red phosphorescent OLEDs reported to date. The high device performance is benefited from the high thermal stability, wide bandgap, efficient energy transfer and the balanced carrier-transport abilities of $Si(PPI)_2$. Our results indicate that $Si(PPI)_2$ is a rare and excellent common host, which may have abilities to simplify the fabrication process and to reduce the material cost in commercial mass production of high-performance multi-color OLEDs. Moreover, $Si(PPI)_2$ will also enable us to design the structurally simple three-primary-color fluorescent/phosphorescent hybrid white OLEDs, which are important and attractive for full-color display and white lighting.

Further application of $Si(PPI)_2$in white OLEDs is ongoing in our lab.

Acknowledgements

Dr. D. Liu and M. Du contributed equally to the work reported in this article. This work was supported by National Basic Research Program of China (2013CB834805), National Natural Science Foundation of China (51173064, 91333201 and 51373062) and Program for Chang Jiang Scholars and Innovative Research Team in University (No.IRT13018).

Notes and references

State Key Laboratory of Supramolecular Structure and Materials College of Chemistry, Jilin University, Changchun 130012, P. R. China E-mail: yuliu@jlu.edu.cn (Y. Liu); zuolun_zhang@yahoo.com.cn (Z. Zhang)

† Electronic Supplementary Information (ESI) available: [photophysical property of compound PPI under same condition]. See DOI: 10.1039/b000000x/

1 C. W. Tang and S. A. VanSlyke, *Appl. Phys. Lett.*, 1987, **51**, 913.
2 M. A. Baldo, D. F. O'Brien, Y. You, A. Shoustikov, S. Sibley, M. E. Thompson and S. R. Forrest, *Nature*, 1998, **395**, 151.
3 M. A. Baldo, S. Lamansky, P. E. Thompson and S. R. Forrest, *Appl. Phys. Lett.*, 1999, **75**, 4.
4 Y. Tao, Q. Wang, C. Yang, Q. Wang, Z. Zhang, T. Zou, J. Qin and D. Ma, *Angew. Chem. Int. Ed.,* 2008, **47**, 8104.
5 S. Watanabe, N. Ide and J. Kido, *Jpn. J. Appl. Phys.*, Part 1 2007, **46**, 1186.
6 T. Peng, S. Huang, K. Q. Ye, Y. Wu, Y. Liu, and Y. Wang, *Org. Electron.*, 2013, **14**, 1649.
7 T. Peng, G. M. Li, K. Q. Ye, C. G. Wang, S. S. Zhao, Y. Liu, Z. M. Hou and Y. Wang, *J. Mater. Chem. C*, 2013, **1**, 2920.
8 F.-M. Hsu, C.-H. Chien, C.-F. Shu, C.-H. Lai, C.-C. Hsieh, K.-W. Wang and P.-T. Chou, *Adv. Funct. Mater.*, 2009, **19**, 2834.
9 C. W. Lee and J. Y. Lee, *Adv. Mater.*, 2013, **25**, 5450.
10 A. Wada, T. Yasuda, Q. Zhang, Y. S. Yang, I. Takasu, S. Enomoto and C. Adachi, *J. Mater. Chem. C*, 2013, **1**, 2404.
11 C. Fan, L. P. Zhu, T. X. Liu, B. Jiang, D. G. Ma, J. G. Qin and C. L. Yang, *Angew. Chem. Int. Ed.,* 2014, **53**, 2147.
12 J.-J. Huang, M.-K. Leung, T.-L. Chiu, Y.-T. Chuang, P.-T. Chou and Y.-H. Hung, *Org. Lett.*, 2014, **16**, 5398.
13 Q. Wang, C.-L. Ho, Y. B. Zhao, D. G. Ma, W.-Y. Wong and L. X. Wang, *Org. Electron.*, 2010, **11**, 238.
14 T. Peng, K. Q. Ye, Y. Liu, L. Wang, Y. Wu and Y. Wang, *Org. Electron.*, 2011, **12**, 1914.
15 T. Peng, G. F. Li, Y. Liu, Y. Wu, K. Q. Ye, D. D. Yao, Y. Yuan, Z. M. Hou and Y. Wang, *Org. Electron.*, 2011, **12**, 1068.
16 Y. Zhang, S. L. Lai, Q. X. Tong, M. F. Lo, T. W. Ng, M. Y. Chan, Z. C. Wen, J. He, K. S. Jeff, X. L. Tang, W. M. Liu, C. C. Ko, P. F. Wang and C. S. Lee, *Chem. Mater.*, 2012, **24**, 61.
17 W. Li, D. Liu, F. Shen, D. Ma, Z. Wang, T. Feng, Y. Xu, B. Yang and Y. Ma, *Adv. Funct. Mater.*, 2012, **22**, 2797.
18 Z. Q. Gao, M. M. Luo, X. H. Sun, H. L. Tam, M. S. Wong, B. X. Mi, P. F. Xia, K. W. Cheah and C. H. Chen, *Adv. Mater.*, 2009, **21**, 688.
19 H. Fukagawa, N. Yokoyama, S. Irisa and S. Tokito, *Adv. Mater.*, 2010, **22**, 4775.
20 Z. Jiang, T. Ye, C. Yang, D. Yang, M. Zhu, C. Zhong, J. Qin and D. Ma, *Chem. Mater.*, 2011, **23**, 771.
21 K. S. Yook and J. Y. Lee, *Adv. Mater.*, 2012, **24**, 3169.
22 S. Y. Shao, J. Q. Ding, T. L. Ye, Z. Y. Xie, L. X. Wang, X. B. Jing and F. S. Wang, *Adv. Mater.*, 2011, **23**, 3570.
23 Q. Wang, J. Q. Ding, D. G. Ma, Y. X. Cheng, L. X. Wang, X. B. Jing and F. S. Wang, *Adv. Funct. Mater.*, 2009, **19**, 84.
24 H.-H. Chou and C.-H. Cheng, *Adv. Mater.* 2010, **22**, 2468.
25 S. Gong, Y. Chen, J. Luo, C. Yang, C. Zhong, J. Qin and D. Ma, *Adv. Funct. Mater.*, 2011, **21**, 1168.
26 Y.–L. Chang, S. Yin, Z. Wang, M. G. Helander, J. Qiu, L. Chai, Z. Liu, G. D. Scholes and Z. Lu, *Adv. Funct. Mater.*, 2013, **23**, 705.
27 Y. Yuan, D. Li, X. Zhang, X. Zhao, Y. Liu, J. Zhang and Y. Wang, *New. J. Chem.* 2011, **35**, 1534.
28 Y. Zhang, S. L. Lai, Q. X. Tong, M. F. Lo, T. W. Ng, M. Y. Chan, Z. C. Wen, J. He, K. S. Jeff, X. L. Tang, W. M. Liu, C. C. Ko, P. F. Wang and C. S. Lee, *Chem. Mater.*, 2012, **24**, 61.
29 W. Li, D. Liu, F. Shen, D. Ma, Z. Wang, T. Feng, Y. Xu, B. Yang and Y. Ma, *Adv. Funct. Mater.*, 2012, **22**, 2797.
30 H. Huang, Y. Wang, S. Zhuang, X. Yang, L. Wang and C. Yang, *J. Phys. Chem. C*, 2012, **116**, 19458.
31 K. Wang, S. P. Wang, J. B. Wei, S. Y. Chen, D. Liu, Y. Liu and Y. Wang, *J. Mater. Chem. C*, 2014, **2**, 6817.
32 K. Wang, S. P. Wang, J. B. Wei, Y. Miao, Y. Liu and Y. Wang, *Org. Electron.*, 2014, **15**, 3211.
33 X. F. Ren, J. Li, R.J. Holmes, P. I. Djurovich, S. R. Forrest and M. E. Thompson, *Chem. Mater.*, 2004, **16**, 4743.
34 S. L. Gong, Q. Fu, Q. Wang, C. L. Yang, C. Zhong, J. G. Qin, D. G. Ma, *Adv. Mater.* 2011, **23**, 4956.
35 Z. Gao, G. Cheng, F. Z. Shen, S. T. Zhang, Y. N. Zhang, P. Lu and Y. G. Ma, *Laser Photonics Rev.*, 2014, **8**, L6.
36 H. Liu, P. Chen, D. H. Hu, X. Y. Tang, Y. Y. Pan, H. H. Zhang,W. Q. Zhang, X. Han, Q. Bai, P. Lu and Y. G. Ma, *Chem. Eur. J.*, 2014, **20**, 2149.
37 D. M. Sun, X. K. Zhou, H. H. Li, X. L. Sun, Y. H. Zheng, Z. J. Ren, D. G. Ma, M. R. Bryce and S. K. Yan, *J. Mater. Chem. C*, 2014, **2**, 8277.
38 Y. G. Ma, P. Lu, Z. M. Wang, Z. Gao, W. J. Li and H. Liu, *Patent*, *CN 102190627 A*, 2011-9-21.
39 T. Peng, H. Bi, Y. Liu, Y. Fan, H. Gao, Y. Wang and Z. Hou, *J. Mater. Chem.*, 2009, **19**, 8072.
40 T. Kumagai and S. Itsuno, *Macromolecules*, 2002, **35**, 5323.
41 C. M. Cardona, W. Li, A. E. Kaifer, D. Stockdale, M. and G. C. Bazan, *Adv. Mater.* 2011, **23**, 2367.
42 Z. Ge, T. Hayakawa, S. Ando, M. Ueda, T. Akiike, H. Miyamoto, T. Kajita and M. Kakimoto, *Adv. Funct. Mater.*, 2008, **18**, 584.
43 Y. T. Tao, Q. Wang, C. L. Yang, C. Zhong, K. Zhang, J. G. Qin and D. G. Ma, *Adv. Funct. Mater.*, 2010, **20**, 304.
44 Z. Ge, T. Hayakawa, S. Ando, M. Ueda, T. Akiike, H. Miyamoto, T. Kajita and M. Kakimoto, *Chem. Mater.*, 2008, **20**, 2532.
45 C. Fan, Y. Chen, Z. Jiang, C. Yang, C. Zhong, J. Qin and D. Ma, *J. Mater. Chem.,* 2010, **20**, 3232.
46 G. M. Li, D. X. Zhu, T. Peng, Y. Liu, Y. Wang and M. R. Bryce, *Adv. Funct. Mater.*, 2014, **24**, 7420.
47 C. W. Tang, S. A. VanSlyke and C. H. Chen, *J. Appl. Phys.*, 1989, **65**, 3610.
48 M. T. Li, W. L. Li, W. M. Su, F. X. Zang, B. Chu, Q. Xin, D. F. Bi, B. Li and T. Z. Yu, *Solid-State Electronics*, 2008, **52**, 121.
49 S. Takizawa, V. A. Montes and P. Anzenbacher Jr., *Chem. Mater.*, 2009, **21**, 2452.
50 T. Peng, G. F. Li, Y. Liu, Y. Wu, K. Q. Ye, D. D. Yao, Y. Yuan, Z. M. Hou and Y. Wang, *Org. Electron.*, 2011, **12**, 1068.
51 T. Peng, K. Q. Ye, Y. Liu, L. Wang, Y. Wu and Y. Wang, *Org. Electron.*, 2011, **12**, 1914.
523 H.-H. Chou, Y.-H. Chen, H.-P. Hsu, W.-H. Chang, Y.-H. Chen and C.-H. Cheng *Adv. Mater.*, 2012, **24**, 5867.
53 H. Fukagawa, T. Shimizu, N. Ohbe, S. Tokito, K. Tokumaru and H. Fujikake, *Org. Electron.*, 2012, **13**, 1197.
54 Z. F. Li, B. Jiao, Z. X. Wu, P. Liu, L. Ma, X. L. Lei, D. G. Wang, G. J. Zhou, H. M. Hu and X. Hou, *J. Mater. Chem. C*, 2013, **1**, 2183.
55 M. R. Zhu and C. L. Yang *Chem. Soc. Rev.,* 2013, **42**, 4963.
56 M.-J. Kim, C.-W. Lee and M.-S. Gong, *Org. Electron.*, 2014, **15**, 2922.
57 T. Komino, H. Nomura, T. Koyanagi and C. Adachi, *Chem. Mater.*, 2013, **25**, 3038.
58 D. Wagner, S. T. Hoffmann, U. Heinemeyer, I. Münster, A. Köhler and P. Strohriegl, *Chem. Mater.* 2013, **25**, 3758.

Graphical Abstract:

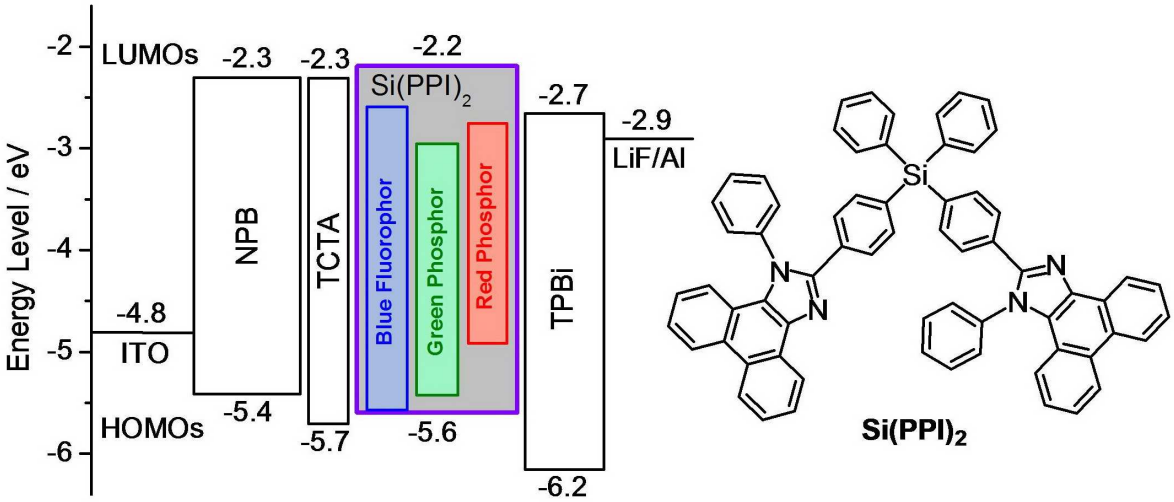

A novel organosilane compound, bis(4-(1-phenylphenanthro[9,10-d]imidazol-2-yl)phenyl)diphenylsilane ($Si(PPI)_2$) with good thermal stability, high-energy emission and good carrier-transport ability, has been designed and synthesized. By using ($Si(PPI)_2$) as a universal host, high-performance fluorescent blue (**FB**) and phosphorescent green (**PG**) and red (**PR**) OLEDs have been achieved. These OLEDs exhibit very high peak external quantum efficiency (EQE) and peak power efficiency (PE), *i.e.* 6.1% & 8.0 lm W^{-1} for **FB** with the CIE coordinates of (0.18, 0.17), 19.2% & 51.1 lm W^{-1} for **PG** and 12.0% & 15.6 lm W^{-1} for **PR**. To the best of our knowledge, the EQE and PE of **FB** are among the highest values ever reported for the pure blue fluorescent OLEDs that meet the standard of the $CIE_{x,y}$ coordinates of $x \leq 0.20$ and $y \leq 0.20$.